Analysis of intrinsic coupling loss in multi–step index optical fibres

Gotzon Aldabaldetreku, Gaizka Durana, Joseba Zubia, Jon Arrue, and Felipe Jiménez

University of the Basque Country,
Alda. Urquijo s/n, E-48013 Bilbao, Spain

gotzon.aldabaldetreku@ehu.es

Javier Mateo

University of Zaragoza,
María de Luna 3, E-50015 Zaragoza, Spain

Abstract: The main goal of the present paper is to provide a comprehensive analysis of the intrinsic coupling loss for multi–step index (MSI) fibres and compare it with those obtained for step– and graded–index fibres. We investigate the effects of tolerances to each waveguide parameter typical in standard manufacturing processes by carrying out several simulations using the ray–tracing method. The results obtained will serve us to identify the most critical waveguide variations to which fibre manufactures will have to pay closer attention to achieve lower coupling losses.

OCIS codes: (060.0060) Fiber optics and optical communications; (060.2270) Fiber characterization; (060.2300) Fiber measurements; (060.2310) Fiber optics.

References and links

1. T. Ishigure, M. Sato, A. Kondo, and Y. Koike, "High–Bandwidth Graded–Index Polymer Optical Fiber with High Temperature Stability," J. Lightwave Technol. **20**, 1443–1448 (2002).
2. I. T. Monroy, H. P. A. van de Boom, A. M. J. Koonen, G. D. Khoe, Y. Watanabe, Y. Koike, and T. Ishigure, "Data transmission over polymer optical fibers," Optical Fiber Technology **9**, 159–171 (2003).
3. K. Irie, Y. Uozu, and T. Yoshimura, "Structure design and analysis of broadband POF," in *Proceedings of the Tenth International Conference on Plastic Optical Fibers and Applications–POF'01*, pp. 73–79 (Amsterdam (The Netherlands), 2001).
4. A. W. Snyder and J. D. Love, *Optical Waveguide Theory* (Chapman and Hall, London, 1983).
5. F. L. Thiel and D. H. Davis, "Contributions of optical–waveguide manufacturing variations to joint loss," Electronic Letters **12**, 340–341 (1976).
6. F. L. Thiel and R. M. Hawk, "Optical waveguide cable connection," Appl. Opt. **15**, 2785–2791 (1976).
7. G. Aldabaldetreku, G. Durana, J. Arrue, M. López-Amo, and J. Zubia, "Measurement of Intrinsic Coupling Loss in Multi–Step Index Optical Fibres," in *13th International Plastic Optical Fibres Conference 2004: Proceedings*, pp. 450–457 (Nuremberg (Germany), 2004).
8. J. Zubia and J. Arrue, "Plastic Optical Fibers: An Introduction to their Technological Processes and Applications," Optical Fiber Technology **7**, 101–140 (2001).
9. S. C. Mettler, "A General Characterization of Splice Loss for Multimode Optical Fibers," Bell Syst. Tech. J. **58**, 2163–2182 (1979).
10. C. M. Miller and S. C. Mettler, "A Loss Model for Parabolic–Profile Fiber Splices," Bell Syst. Tech. J. **57**, 3167–3180 (1978).
11. D. J. Bond and P. Hensel, "The effects on joint losses of tolerances in some geometrical parameters of optical fibres," Optical and Quantum Electronics **13**, 11–18 (1981).
12. Mitsubishi Rayon Co., Ltd.: "Eska–Miu," URL http://www.pofeska.com.
13. V. Levin, T. Baskakova, Z. Lavrova, A. Zubkov, H. Poisel, and K. Klein, "Production of multilayer polymer optical fibers," in *Proceedings of the Eighth International Conference on Plastic Optical Fibers and Applications–POF'99*, pp. 98–101 (Chiba (Japan), 1999).

#6600 - $15.00 US Received 14 February 2005; revised 13 April 2005; accepted 17 April 2005

14. D. Marcuse, *Principles of Optical Fiber Measurements*, chap. 4 (Academic Press, Inc., London, 1981).
15. Japanese Standards Association, "Test methods for structural parameters of all plastic multimode optical fibers," Tech. Rep. JIS C 6862, JIS, Tokyo, Japan (1990).
16. J. Zubia, G. Aldabaldetreku, G. Durana, J. Arrue, H. Poisel, and C. A. Bunge, "Geometric Optics Analysis of Multi–Step Index Optical Fibers," Fiber and Integrated Optics **23**, 121–156 (2004).

1. Introduction

The feasibility of multi–step index (MSI) fibres is currently under consideration because they could serve as a complement to glass fibres or high–bandwidth graded–index polymer optical fibres (GI–POF) [1, 2] in short–haul communications links. This is due to the simpler processes involved in the manufacturing of this type of fibres, as well as to the better stability of their refractive index profiles with ageing, temperature fluctuations and humidity changes. Furthermore, they combine the simplicity of their step–index (SI) counterparts in manufacturing and the higher bandwidths achievable with graded–index (GI) fibres, to the point of allowing, using an MSI polymer optical fibre (MSI–POF) of three layers with a numerical aperture (*NA*) of 0.25, for instance, bandwidths as high as 250 MHz $\cdot$ 100 m [3].

The insertion loss of a fibre splice or a connector is the primary measure of its quality. For this reason, in the process of splicing or in the design of a connector it is of critical importance to understand and evaluate the sources of loss in fibre–to–fibre coupling, which are classified as extrinsic and intrinsic coupling losses.

Although the extrinsic coupling losses can be controlled and cancelled or at least minimized to a practically negligible value by improving the fibre joining techniques, all methods continue to have intrinsic contributions to loss. The intrinsic coupling losses arise from the inevitable variations in waveguide properties as a result of standard manufacturing processes, which affect the light propagation characteristics of the fibres being joined. Therefore, this paper investigates the effects of tolerances to the surface diameter of each core, the axial eccentricity between each core and cladding (i.e., the deviation of the concentricity between them), their circular eccentricity (or ellipticity), and the numerical aperture.

This will be accomplished by carrying out simulations using the ray–tracing method [4], since the results obtained are not only more realistic, as they include more effects susceptible to cause further losses, but also they take advantage of not relying on assumptions used in the analytical expressions of the common mode volume, and they are not restricted to mismatches only in core diameters or numerical apertures [5, 6, 7].

The structure of the paper is as follows. First of all, we carry out several simulations for the SI fibre and the clad parabolic profile GI fibre using the ray–tracing method, measuring intrinsic coupling losses separately when each of the waveguide parameters varies at discrete steps, which is useful to appreciate the amount of control required on them. The results obtained will serve us to identify the most critical parameters. Afterwards, we perform a statistical analysis of the intrinsic coupling loss for the same fibres. This task will be carried out by running a set of computer simulations which involve joining two fibres randomly chosen from a given population following a normal distribution. The results obtained will serve us to check whether the most critical structural parameters concluded from the analysis in which coupling losses were measured with discrete variations of each of them are the same or not, as well as to compare intrinsic coupling losses of different types of MSI fibres. These fibres are analysed from a statistical point of view in a subsequent section and the results obtained for them are discussed. Finally, we summarize the main conclusions.

#6600 - $15.00 US Received 14 February 2005; revised 13 April 2005; accepted 17 April 2005

2. Analysis of the simulation results obtained by using the ray–tracing method for SI and GI fibres

In this section we will identify the most critical waveguide parameters and evaluate the intrinsic coupling loss for SI and clad parabolic profile GI fibres by performing several computer simulations using the ray–tracing method.

We have chosen the value of 1.492 as the highest refractive index in the core ($n(0) = n_{co}$) and 1.402 as the refractive index of the cladding (n_{cl}), yielding a peak numerical aperture ($NA(0)$) of 0.51 for the transmitting fibre. Let the radius of the core of the transmitting fibre be $\rho = 380\,\mu$m. These values can be arbitrarily chosen, since each of the fibre parameter variations is normalized to its respective parameter and, therefore, the results obtained are the same, even if the fibre dimensions or the material properties are scaled to greater or lower values (in the framework of the classical geometric optics). Furthermore, it should be emphasized that although the simulations were carried out using characteristics typical of POFs [8], the obtained results are valid for any kind of highly multimode optical fibre used as a transmission medium.

For the sake of simplicity, we will not pay attention to the possible effects of the protective jacket and assume that the cladding extends to infinity.

We have launched 180000 rays from a hypothetical source covering the whole input surface of the transmitting fibre and emitting a uniform mode distribution (UMD) with a numerical aperture $NA_{input} = 0.57$ (thus, ensuring that the launched rays will fill the effective solid acceptance angle of the transmitting fibre).

2.1. Determination of the most critical waveguide parameters and their effect on the intrinsic coupling loss

Figures 1 and 2 show the results obtained for the intrinsic coupling losses of the SI fibre and the clad parabolic profile GI fibre, when each of the waveguide parameters of the receiving fibre varies at discrete steps between -5% and $+5\%$ of its reference value set by the transmitting fibre (or between 0 and a maximum circular eccentricity of 0.5, where appropriate). As can be seen in Figs. 1(a) and 2(a), the numerical aperture and the core diameter are the most critical parameters, whereas the axial eccentricity of each core and cladding and their circular eccentricity are the least critical ones (see Figs. 1(b) and 2(b)). It should also be pointed out that, for nearly clad parabolic profile GI fibres, mismatches in their refractive index profile exponents lead to lower coupling losses, as can be observed in Figs. 2(c) and 2(d) [9, 10]. However, since this effect cannot occur in SI fibres, we will give little heed to this kind of mismatch.

Let us now turn our attention to Figs. 1(a) and 2(a), which correspond to the coupling loss attributable to numerical aperture and core diameter mismatches for SI and clad parabolic profile GI fibres, respectively. On the one hand, it can be observed that the coupling loss for a clad parabolic profile GI fibre is approximately 0.24 dB lower than that for an SI one when considering that the radius of the receiving fibre ρ_r is 5% larger than that of the transmitting fibre ρ_t and assuming a peak numerical aperture of the receiving fibre ($NA_r(0)$) 5% lower than that of the transmitting fibre ($NA_t(0)$).

In order to be able to understand the reason for such a behaviour, we have to refer to the near– and far–fields of the transmitting fibre for both SI and clad parabolic profile GI fibres. It turns out that the probability of having very tilted rays (those closest to the critical angle) is equiprobable at any position of the SI fibre core, whereas in clad parabolic profile GI fibres this kind of very tilted rays can only propagate close to the fibre centre, in accordance with the clad parabolic profile (where the numerical aperture decreases with the radial position following a parabolic power–law), which results in a lower fraction of power emitted at the outermost radial positions of the clad parabolic profile GI fibre.

Taking this into account, the better results obtained for the clad parabolic profile GI fibres

#6600 - $15.00 US Received 14 February 2005; revised 13 April 2005; accepted 17 April 2005

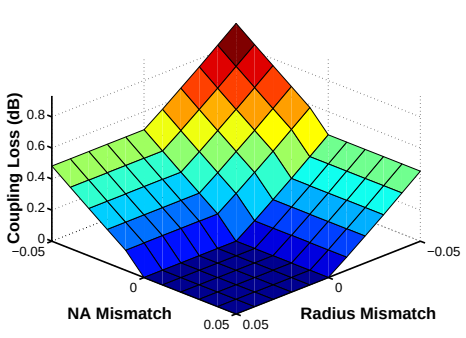

(a) Numerical aperture vs radius.

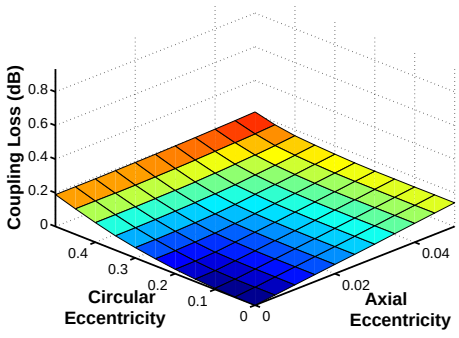

(b) Circular eccentricity vs axial eccentricity.

Fig. 1. Simulation results for the intrinsic coupling loss for tolerances of ±5% and a maximum circular eccentricity of 0.5 by using the ray–tracing method. Results obtained for the SI fibre (only the most significant combinations). All the parameters have been normalized.

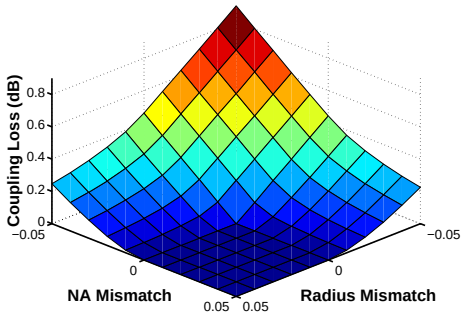

(a) Numerical aperture vs radius.

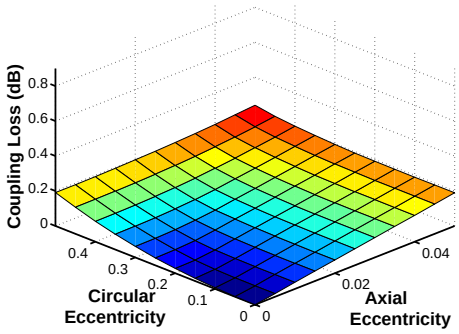

(b) Circular eccentricity vs axial eccentricity.

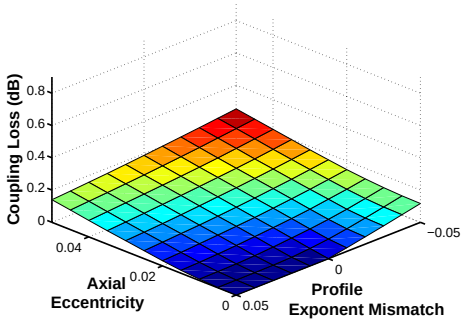

(c) Axial eccentricity vs profile exponent.

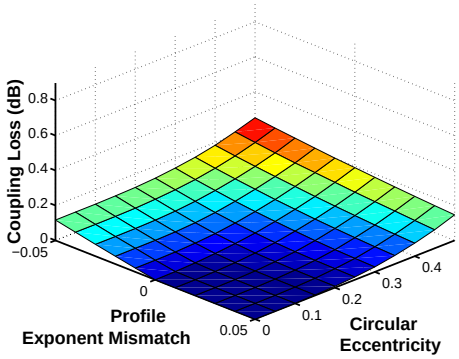

(d) Profile exponent vs circular eccentricity.

Fig. 2. Simulation results for the intrinsic coupling loss for tolerances of ±5% and a maximum circular eccentricity of 0.5 by using the ray–tracing method. Results obtained for the clad parabolic profile GI fibre (only the most significant combinations). All the parameters have been normalized.

#6600 - $15.00 US
Received 14 February 2005; revised 13 April 2005; accepted 17 April 2005

demonstrate a kind of compensation effect, because the most external surface of the receiving fibre having the lowest numerical aperture stands outside the area covered by the transmitting one due to the greater diameter of the receiving fibre, and therefore, the proportion of power collected by the receiving fibre at the boundaries of the transmitting one is greater than it would be if both fibres had the same core diameter. This compensation does not occur in an SI fibre, since its numerical aperture remains constant across the core. Similarly, if we now consider, in relation to the transmitting fibre, that the radius of the receiving fibre ρ_r is 5% smaller, but with a peak numerical aperture $NA_r(0)$ that is 5% higher, then the coupling loss for a clad parabolic profile GI fibre turns out to be approximately 0.23 dB lower than that for an SI one.

In any case, it is clearly noticeable that the way the coupling loss vary with each of the mismatches is different for each kind of fibre, since in most cases the change in an SI fibre is almost linear, whereas in a GI one it follows a quasi–parabolic shape, which is consistent with the parabolic dependence exhibited by its numerical aperture.

On the other hand, it is particularly interesting to compare the results of the coupling loss for both SI and clad parabolic profile GI fibres when the numerical aperture and core diameter mismatches are considered separately and in the most unfavourable cases (that is, either considering that the radius of the receiving fibre ρ_r is 5% lower than that of the transmitting fibre ρ_t while maintaining the peak numerical apertures unchanged, or considering that the peak numerical aperture of the receiving fibre $NA_r(0)$ is 5% lower than that of the transmitting fibre $NA_t(0)$ while maintaining the diameters unchanged). The results show that there are no appreciable differences between SI and GI fibres (the coupling loss attributable to mismatches in core diameters is in the order of 0.48 dB for an SI fibre and 0.46 dB for a GI one, whereas the coupling loss attributable to mismatches in numerical apertures yields 0.45 dB for an SI fibre and 0.44 dB for a GI one).

If we take the first case (core diameter mismatch with unchanged peak numerical apertures), from the examination of the the near– and far–fields of the transmitting fibre, it can be deduced that the fraction of power lost in the SI case is just that emitted by the most external ring of the transmitting fibre that lies outside the limits of the receiving one. The power emitted by the rest of the inner surface of the transmitting fibre (which covers the whole input surface of the receiving fibre) is collected entirely by the receiving fibre without incurring further losses. Conversely, as already explained, in a clad parabolic profile GI fibre the fraction of power emitted at its outermost positions is much lower than that in an SI one so, in principle, the incurred losses should be lower; nevertheless, and in contrast to what happened with SI fibres, the receiving fibre does not collect entirely the power emitted by the inner surface of the transmitting fibre, because the radial dependence of the acceptance angle of the latter has changed in relation to that shown by the former, in spite of the peak numerical aperture not having varied. As a consequence, there is an additional source of losses which in the end leads to very similar results as those obtained in the case of SI fibres. The same reasoning holds if we take the second case in which the peak numerical aperture of the receiving fibre experienced a mismatch of 5% lower with unchanged core diameters.

2.2. Statistical analysis of the intrinsic coupling loss in SI and GI fibres

Additionally, we have also evaluated the intrinsic coupling losses from a statistical point of view for the sake of comparison with the results obtained for MSI fibres in section 3. Using the ray–tracing method, we have run a set of computer simulations of 5000 trials that involve joining two fibres randomly chosen from a given population following a normal distribution, in order to confirm that the most critical parameters coincide with those predicted in subsection 2.1.

Figure 3 shows the results obtained for the coupling loss when only one of the possible parameters is varied and also when the mismatches are applied all together for the SI and clad

#6600 - $15.00 US Received 14 February 2005; revised 13 April 2005; accepted 17 April 2005

parabolic profile GI fibres. The ordinate shows the cumulative percentage of fibre joints which have intrinsic coupling losses lower than the value given in the abscissa. The values chosen for their parameters are the same as those used in the analysis in which coupling losses were measured with discrete variations of each of the structural parameters of the receiving fibre. Each parameter has a normalized standard deviation of 5% (or a value of 0.268 in the case of the circular eccentricity mismatch).

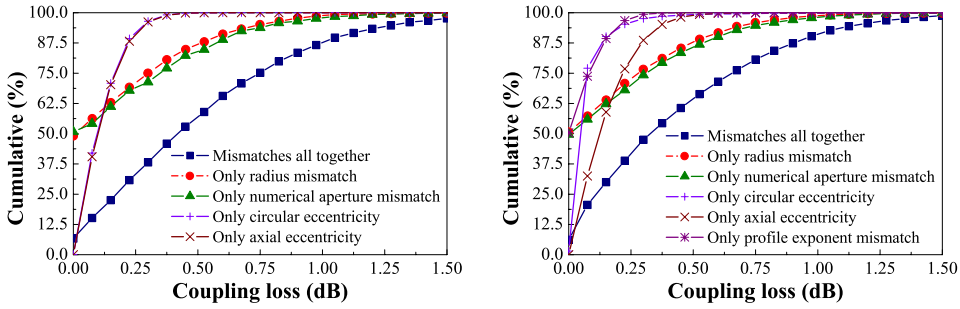

(a) SI fibre. (b) GI fibre.

Fig. 3. Cumulative percentage of fibre joints having intrinsic coupling losses below a given value. Results obtained for simulations of 5000 trials and for SI and clad parabolic profile GI fibres by using the ray–tracing method.

The details of the 50% loss or median loss L_{50} and the 90% loss L_{90} are shown in Table 1. The 50% loss L_{50} denotes that 50% of the samples considered in a large statistical population of fibres following a normal distribution will have intrinsic coupling losses below such a loss value (L_{50}). The same applies to the 90% loss L_{90}.

Table 1. Statistical results obtained for the 50% loss L_{50} and the 90% loss L_{90} for SI and clad parabolic profile GI fibres by using the ray–tracing method.

	SI fibre		**GI fibre**	
	L_{50}(dB)	L_{90}(dB)	L_{50}(dB)	L_{90}(dB)
Mismatches all together	0.418	1.056	0.325	0.966
Only radius mismatch	0.008	0.57	0.0	0.55
Only numerical aperture mismatch	0.0	0.62	0.002	0.595
Only circular eccentricity	0.091	0.23	0.022	0.148
Only axial eccentricity	0.095	0.236	0.121	0.312
Only profile exponent mismatch	–	–	0.0	0.154

It should be kept in mind that the use of normally distributed random deviations would in principle make it possible for occasional too extreme parameters to be generated in the computer simulations which would not be encountered in practice, although the probability of obtaining such parameters is virtually negligible. For instance, the probability of coming across a random deviation within four standard deviations is of 99.994% (notice that for the normalized standard deviations chosen for each parameter, the corresponding percentile value of the mismatch is of $4 \times 0.05 = 0.2 = 20\%$). Therefore, the probability of obtaining a random deviation outside the same interval is of only 0.006%, so we can only expect to find approximately

#6600 - $15.00 US Received 14 February 2005; revised 13 April 2005; accepted 17 April 2005

fewer than 0.3 samples, i.e. practically no samples, exceeding the value of this mismatch after each set of computer simulations of 5000 trials. Likewise, we can calculate the percentile value corresponding to the limit points of the interval of the probability function out of which, statistically, only one sample out of 5000 trials is expected. This turns out to be equal to 3.719 standard deviations, that is, 18.595%. These percentile values, though certainly high, are still perfectly plausible.

The choice of the normalized standard deviation in the case of the circular eccentricity mismatch e deserves careful consideration. Taking into account that the values for the circular eccentricity must be by definition in the interval $[0,1)$ (since $e = \left(1 - b^2/a^2\right)^{1/2}$, being a the fibre major semi–axis and b the fibre minor semi–axis), a suitable value has to be chosen so that the probability of obtaining a random deviation outside the allowed interval will be low enough to avoid eccentricities greater than one, which can be achieved if the expected number of samples exceeding the maximum allowed value after each set of computer simulations of 5000 trials is fewer than one. In this case, a normalized standard deviation of 0.268 assures the previous requirement.

At first sight, it can be noted, both in Fig. 3(a) and in 3(b), that when considering all the mismatches taking place simultaneously, the coupling loss is the highest one, whereas with only one mismatch, the most critical parameters are the numerical aperture and the core diameter, in good agreement with Figs. 1(a) and 2(a) (in the case of the clad parabolic profile GI fibre, when only mismatches in refractive index profile exponents occur, the coupling loss is even lower, in the same way as in Figs. 2(c) and 2(d)). On closer examination it is found that the coupling loss when considering the mismatches all together is neither the sum of the coupling losses due to each parameter variation (which would lead to too pessimistic values) nor the quadratic mean of them (which would instead lead to quite optimistic results), since some effects may cancel each other out. In any case, the general behaviour of the coupling loss remains the same, in the sense of being higher for SI fibres than for GI ones.

By considering the circular eccentricity and the axial eccentricity of core and cladding separately, we can again observe in Fig. 3 that they are indeed the least critical parameters in terms of intrinsic coupling losses, in the same way as suggested by Figs. 1(b) and 2(b), although the statistical results gathered in Table 1 are apparently quite contradictory. Indeed, the 50% losses L_{50} for the circular and axial eccentricities are certainly higher than those obtained for the most critical parameters separately, whereas only the results obtained for the 90% loss L_{90} seem to confirm the conclusions drawn in subsection 2.1. In order to understand the reason for having such results, we have to analyse the implications of using random deviations following a normal distribution.

As to the coupling loss results obtained when the numerical aperture and core diameter mismatches were considered separately, it is necessary to bear in mind that we have the same probabilities of coming across a positive or negative random deviation. A negative deviation (meaning that the receiving fibre has a lower numerical aperture or a smaller core diameter) incurs losses, whereas a positive one leads to no loss at all – similar results apply to variations in the refractive index profile exponent g of the clad parabolic profile GI fibre. However, for the circular and axial eccentricities, the only way of having no loss is to come across with a null deviation, or in other words, even a positive random deviation incurs coupling loss when dealing with eccentricities instead of mismatches. For this reason, it is expected that the median loss L_{50} obtained for the latter will be more optimistic than that for the former, though the 90% loss L_{90} will reveal us that indeed the numerical aperture and core diameter are the most critical parameters.

This statement is also reinforced by considering the following fact: even though the effects on the intrinsic coupling losses of mismatches in circular eccentricities ranging in the interval

#6600 - $15.00 US Received 14 February 2005; revised 13 April 2005; accepted 17 April 2005

$[0.5,1)$ can be considerably adverse, especially for values exceeding 0.9 and although in our statistical analysis at least about 6.296% of the samples of the total number of trials lies in this range (i.e., approximately 315 samples out of 5000 trials or 4 samples exceeding 0.9 out of 5000), we can observe that their effect on the coupling loss is not as significant as in the case of the numerical aperture and core diameter mismatches. This is noticeable in Figs. 3(a) and 3(b).

Finally, it must be pointed out that, in the case of the SI and the clad parabolic profile GI fibres, the different approaches used in the random trials have hardly any effect on the incurred coupling losses. For the analysis in which the circular eccentricity and the axial eccentricity varied at discrete steps between 0 and a maximum of 0.5 and between 0% and +5%, respectively, the angle that describes the orientation of the fibre [11], that is to say, the angle between the major fibre semi–axis and the reference offset direction, was always fixed to zero and both the transmitting and receiving fibre axes were always displaced transversely along the same direction. In contrast, for the statistical analysis of the intrinsic coupling loss, such angle was randomly chosen from a uniform distribution. Because of the circular symmetry of the fibre, the latter will have no effect on the coupling loss in comparison with the former, as long as each of the mismatches takes place separately (however, we will see in section 3 that the constraints imposed by the use on each layer of the MSI receiving fibre of different uniformly random angular deviations will have an important effect on the obtained results).

3. Analysis of the simulation results obtained by using the ray–tracing method for MSI fibres

In this section we have carried out several simulations for three different MSI fibres using the ray–tracing method. The details concerning the characteristics of the chosen fibres are presented below.

3.1. Properties of the examined MSI fibres

MSI fibres are structurally very similar to their SI or GI counterparts, since they consist of a core, a cladding that surrounds the core, and a protective jacket covering the cladding. However, the main difference arises from the fact that the core consists of several layers of different refractive indices. The most general refractive index profile in MSI fibres can be expressed as

$$n(r) = \begin{cases} n_1; & r < \rho_1, \\ n_2; & \rho_1 \leqslant r < \rho_2, \\ \vdots & \\ n_N; & \rho_{N-1} \leqslant r < \rho_N, \\ n_{cl}; & r \geqslant \rho_N. \end{cases} \tag{1}$$

Taking into account that an MSI fibre can be used as an approach of any kind of GI fibre, provided that it has a sufficiently high number of layers N, we have chosen a parabolic profile MSI fibre of $N = 10$ layers to be able to compare the intrinsic coupling loss results obtained for this fibre with those obtained in subsection 2.2 for the clad parabolic profile GI fibre. This is achieved by maintaining the width of each layer constant (i.e., $\rho_i - \rho_{i-1} = \text{constant} \quad \forall i$) and fitting the refractive indices of the MSI fibre in such a way that the overall refractive index profile approximates to that of the GI fibre:

$$n_{MSI,i} = n_{GI}(r)\Big|_{r=\rho_{i-1}} \qquad \forall i.$$

Furthermore, in order to evaluate statistically the influence of the intrinsic coupling loss on the performance of real MSI fibres, we have taken two different MSI–POFs: the Eska–Miu

#6600 - $15.00 US Received 14 February 2005; revised 13 April 2005; accepted 17 April 2005

fibre from Mitsubishi [12], and the MSI–POF from TVER [13]. The former has three layers, the innermost one being fairly thick and the outermost one extremely thin, whereas the latter has four layers, three of them of similar thickness. The physical dimensions of the different layers are reproduced in Table 2. Figures 4(a) and 4(b) show, in addition, their respective refractive index profiles measured with the aid of the inverse near–field method [14, 15].

Table 2. Physical dimensions of the different layers (radii in mm).

	Layer 1	Layer 2	Layer 3	Layer 4
Eska–Miu	0.25	0.35	0.38	–
TVER	0.16	0.23	0.27	0.33

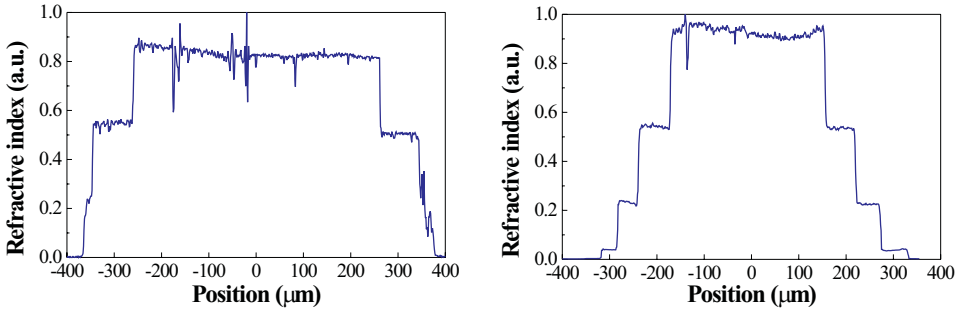

(a) Eska–Miu fibre. (b) TVER fibre.

Fig. 4. Refractive index profiles corresponding to the two MSI–POFs used.

3.2. Statistical analysis of the intrinsic coupling loss in MSI fibres

First of all, it must be kept in mind that the study of MSI fibres is complicated by the fact that they consist of several layers, which means that the number of parameters that are liable to vary multiply as the number of layers increases, making it difficult to carry out analyses like in subsection 2.1, if not impossible.

For this reason, we have tackled the evaluation of intrinsic coupling losses for MSI fibres from a statistical point of view by running computer simulations of 5000 trials when joining two fibres randomly chosen from a given population following a normal distribution.

Once again we have utilized a hypothetical source that covers the whole input surface of the transmitting fibre, which emits a UMD with a numerical aperture of $NA_{input} = 0.57$. On each trial, we have launched 200000, 115000 or 235000 rays into Eska–Miu fibres, TVER fibres or parabolic profile MSI fibres of $N = 10$ layers, respectively.

Figure 5 shows the results obtained for the intrinsic coupling loss when only one of the parameters is varied and also when the mismatches are applied all together, considering the Eska–Miu and the TVER MSI–POFs, as well as the parabolic profile MSI fibre of $N = 10$ layers whose parameters are $NA_{1,t} = 0.51$ and $\rho_{10,t} = 490\ \mu$m (the selection of these values does not impose any restriction on the obtained results, since each of the fibre parameter variations is normalized separately). Each parameter has a normalized standard deviation of 5% (or a value of 0.268 in the case of the circular eccentricity). The details of the 50% loss or median loss L_{50} and the 90% loss L_{90} for each type of fibre are shown in Table 3.

#6600 - $15.00 US Received 14 February 2005; revised 13 April 2005; accepted 17 April 2005

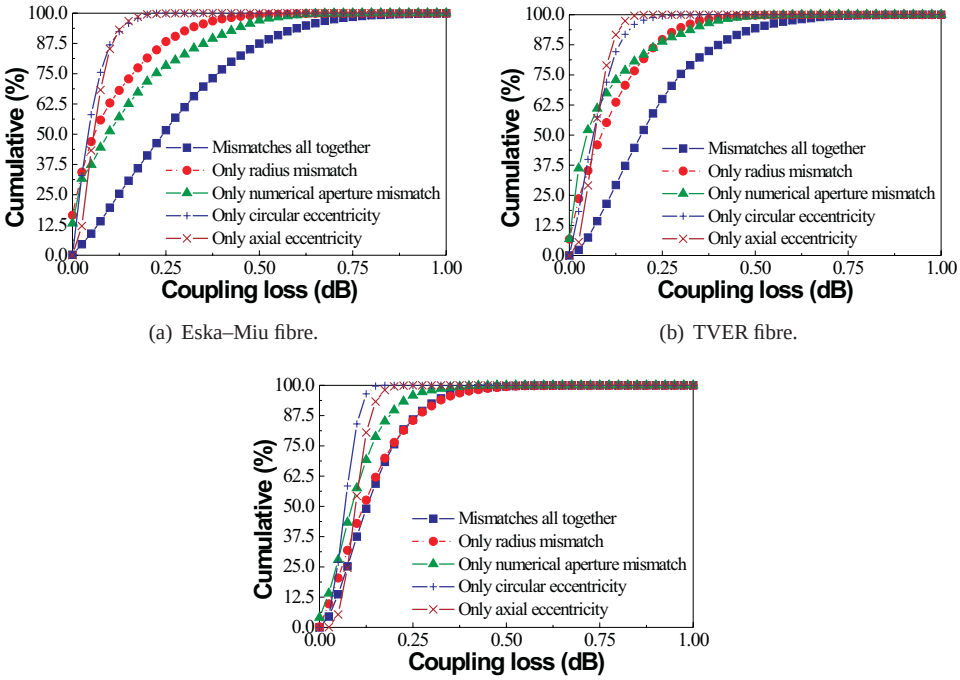

(a) Eska–Miu fibre.

(b) TVER fibre.

(c) Parabolic profile MSI fibre ($N = 10$).

Fig. 5. Cumulative percentage of fibre joints having intrinsic coupling losses below a given value. Results obtained for simulations of 5000 trials and for different MSI fibres by using the ray–tracing method.

Table 3. Statistical results obtained for the 50% loss L_{50} and the 90% loss L_{90} for different MSI fibres by using the ray–tracing method.

	Eska–Miu fibre		**TVER fibre**	
	L_{50}(dB)	L_{90}(dB)	L_{50}(dB)	L_{90}(dB)
Mismatches all together	0.241	0.535	0.191	0.428
Only radius mismatch	0.057	0.269	0.084	0.252
Only numerical aperture mismatch	0.096	0.38	0.046	0.267
Only circular eccentricity	0.039	0.111	0.063	0.141
Only axial eccentricity	0.055	0.113	0.068	0.12

Parabolic profile MSI fibre (N = 10)		
	L_{50}(dB)	L_{90}(dB)
Mismatches all together	0.126	0.28
Only radius mismatch	0.117	0.283
Only numerical aperture mismatch	0.086	0.201
Only circular eccentricity	0.068	0.109
Only axial eccentricity	0.096	0.14

#6600 - $15.00 US
Received 14 February 2005; revised 13 April 2005; accepted 17 April 2005

The procedure for the random building of the receiving fibre on each trial is as follows: firstly, the innermost layer of the receiving fibre is built in accordance with a certain radius, a circularity deviation and an axial eccentricity, all of them following a normal random distribution, taking as the mean values those corresponding to the innermost layer of the transmitting fibre. As for the angle that describes the orientation of the innermost layer, this is randomly chosen from a uniform distribution. Its numerical aperture is also randomly chosen from a normal distribution, independently of the rest of the parameters. In all cases, when a negative parameter value has been mathematically generated, the trial is aborted and a new receiving fibre is built using new random choices.

Afterwards, the next layers surrounding the innermost ones are sequentially generated randomly in a similar way, the mean values now corresponding to their respective layers of the transmitting fibre. The angles that describe the orientation of each layer of the receiving fibre and the polar angles related to the transverse offset direction between the corresponding layer axes are randomly chosen from a uniform distribution. Special care must be taken so that only positive parameter values will be accepted, avoiding overlapping of layers in which an inner layer radius results to be larger than that of a surrounding one and assuring that the numerical aperture continually decreases towards the exterior. Otherwise, the trial is aborted and a new receiving fibre is built from the beginning using new random choices. Although, mathematically, absurd parameters could be encountered, the previous condition prevents this kind of situations from happening.

It is of fundamental importance to bear in mind that the realistic constraints imposed on the building of the receiving fibre will have a relatively large effect on the obtained results, their effects being more dramatic as the number of layers increases. Specifically, the more layers an MSI fibre has, the narrower the accepted margins are, which leads to a conservative estimate of the coupling efficiency.

From Fig. 5 it is noticeable that the numerical aperture and the core diameter are the most critical parameters, in the same way as happened with SI and clad parabolic profile GI fibres in section 2. However, now it is evident that the coupling loss results are quantitatively lower than those obtained for SI and clad parabolic GI fibres (as can be deduced from the value of the 90% loss L_{90} in Table 3), especially in the case of the coupling loss due to mismatches in circular eccentricities. This is due to the numerous truncations, for instance, forced those by having used different random angles on each layer of the MSI fibres for the circular eccentricity, which results in a much lower proportion of layers having high circular eccentricity values and, therefore, in lower coupling losses.

Figures 5(a) and 5(b) show that the coupling loss for the TVER fibre is slightly lower than that for the Eska–Miu fibre (which has one layer less); the coupling loss for the parabolic profile MSI fibre of $N = 10$ layers is even much lower than that for the Eska–Miu or the TVER fibres, as can be seen in Fig. 5(c). This result is consistent with the fact that the number of layers of an MSI fibre has some slight influence on the coupling loss (as was reported in Ref. [7]), but it is rather surprising because of its unusual low value, especially if we compare this with the results obtained for the clad parabolic profile GI fibre (see Fig. 3(b)) discussed in section 2.

In the same way as in subsection 2.1, we have to analyse the near– and far–fields of the transmitting fibre shown in Fig. 6 for the MSI–POFs discussed if we want to find a satisfactory explanation of why the parabolic profile MSI fibre of $N = 10$ layers experiments such a great improvement in terms of intrinsic coupling losses.

It can be observed from direct comparison between the sets of Figs. 6(e), 6(a), 6(c) and Figs. 6(f), 6(b), 6(d) that the particular near– and far–fields emitted by the transmitting parabolic profile MSI fibre of $N = 10$ layers are dependent on the type of MSI–POF. These far–fields are the direct consequence of the number of layers this consists of, as well as of the geometric

#6600 - $15.00 US Received 14 February 2005; revised 13 April 2005; accepted 17 April 2005

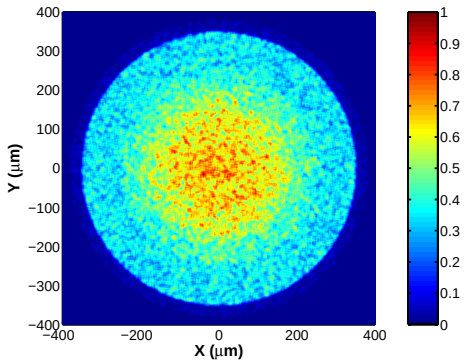

(a) Near–field for the Eska–Miu fibre.

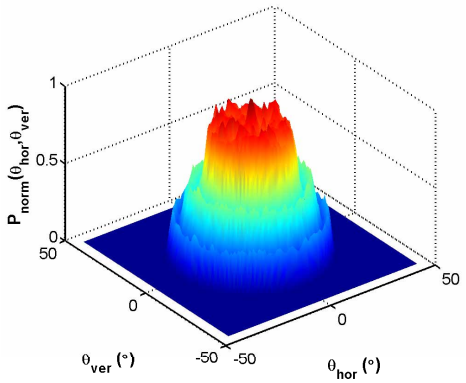

(b) Far–field for the Eska–Miu fibre.

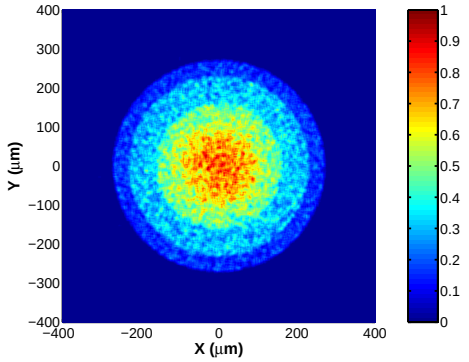

(c) Near–field for the TVER fibre.

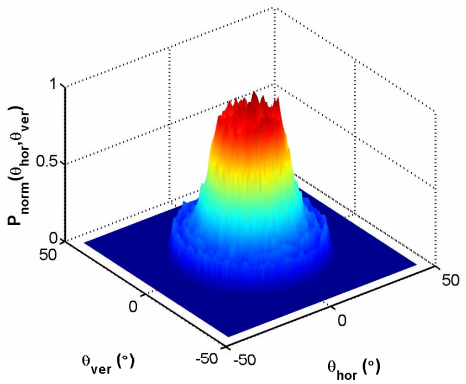

(d) Far–field for the TVER fibre.

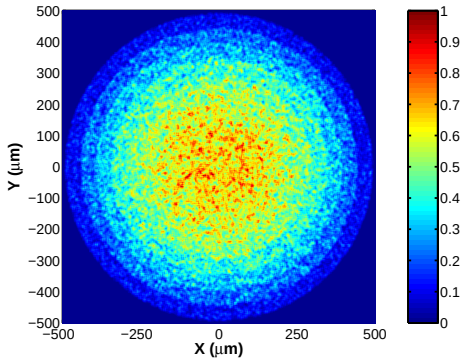

(e) Near–field for the parabolic profile MSI fibre ($N = 10$).

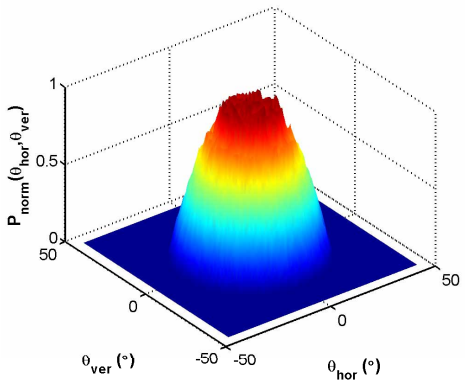

(f) Far–field for the parabolic profile MSI fibre ($N = 10$).

Fig. 6. Near– and far–fields of the transmitting fibre with $NA_{input} = 0.57$ in the computer simulations for MSI fibres.

#6600 - $15.00 US Received 14 February 2005; revised 13 April 2005; accepted 17 April 2005

arrangement of these layers and the overall refractive index profile. These characteristics are certainly advantageous in terms of keeping the coupling loss at lower values than those obtained for the Eska–Miu and the TVER fibres (the TVER fibre exhibits similar though slightly better results than the Eska–Miu fibre, as well), for the same reasons already discussed.

Finally, it would be very convenient to take into account that the gain in having such an enhancement with the parabolic profile MSI fibre of $N = 10$ layers can also be spoiled by the fact that the source power collected by the transmitting fibre drops. Indeed, if we considered the case of a diffuse illumination and calculated the theoretical source efficiencies for each MSI fibre by using the formula [16]

$$\xi = \frac{\sum_{i=1}^{N} \left(\rho_i^2 - \rho_{i-1}^2\right)\left(n_i^2 - n_{cl}^2\right)}{n_0^2 \rho_N^2} \qquad (\rho_0 = 0), \tag{2}$$

we would obtain the following results, ranked in descending order: $\xi_{\text{Eska–Miu}} = 0.194$ or -7.12 dB, $\xi_{\text{Parabolic profile MSI Fibre } N=10} = 0.1476$ or -8.31 dB, and $\xi_{\text{TVER}} = 0.1152$ or -9.38 dB.

Therefore, the launched power is better coupled into the Eska–Miu fibre than into the parabolic profile MSI fibre of $N = 10$ layers or into the TVER fibre, the differences ranging from 1.07 to 2.26 dB between each other. These values are definitely far more significant than the improvement that would be obtained if we only had taken into account the incurred coupling loss when taking place the parameter mismatches all together (being the highest difference of 0.141 dB for the median loss L_{50} and of 0.325 dB for the 90% loss L_{90}, as can be extracted from Table 3).

The same applies to the SI and clad parabolic profile GI fibres, where the SI fibre shows a higher source efficiency in comparison with the clad parabolic profile GI fibre ($\xi_{\text{SI}} = 0.26$ or -5.85 dB whereas $\xi_{\text{GI}} = 0.13$ or -8.85 dB).

4. Conclusion

We have statistically analysed the quantitative effects that each waveguide variation has on the coupling loss for SI, clad parabolic profile GI and three different MSI fibres. We have also identified the most and least critical waveguide parameters in terms of intrinsic coupling losses. Finally, in the light of the results, it is clear that fibre manufacturers will have to pay close attention to the variations in the refractive indices and the diameters of the layers from which the core of the fibre is compounded, in order to reduce intrinsic coupling losses as much as possible.

Acknowledgments

The authors would like to thank T. Yamamoto of Mitsubishi Rayon Co., Ltd. and Prof. V. Levin of RPC for supplying the MSI–POF samples, and also Prof. H. Poisel of the University of Applied Sciences of Nuremberg for many fruitful discussions.

This work was supported by the *Universidad del País Vasco–Euskal Herriko Unibertsitatea* and the *Ministerio de Ciencia y Tecnología* under projects 9/UPV 00147.345-14626/2002ZUBIA, and TIC2003-08361.